

RESEARCH ARTICLE

Optimization of Bench Width and Vertical Bench Position for Claystone Slopes Using the Limit Equilibrium Method under a Safety Factor Constraint

Kyrie Eleison Putra¹, Fariz Aditya^{1,*}, Bambang Heriyadi¹, Rudy Anarta¹

¹ Mining Engineering Department, Universitas Negeri Padang, Jl. Prof. Dr. Hamka, Padang, West Sumatera, Indonesia

* Corresponding author : farizaditya@unp.ac.id
Tel.: +62 813 631 04 085
Received: Apr 27, 2026; Accepted: Jun 08, 2026.
DOI: 10.25299/jgeet.2026.11.02.28001

Abstract

One important aspect of open pit mine planning is slope geometry design, which affects the stability of the slope and the efficiency of overburden removal. This study aims to investigate the influence of vertical bench position and bench width on slope stability and their effect on stripping volume. The limit equilibrium method was used for slope stability analysis, with the assistance of Rocscience Slide2 software. The stripping volume estimate was obtained from pit shell simulations using GEOVIA Surpac software. The vertical bench positions analyzed were $\frac{1}{4}$, $\frac{1}{2}$, and $\frac{3}{4}$ of the total slope height, which was 60 m. The bench width variations tested were 0, 5, 10, 15, 20, and 25 m, while maintaining a minimum safety factor requirement of 1.3. The analysis indicated that the optimal configuration is achieved by placing the bench at the vertical position of $\frac{1}{2}$ of the overall slope height with a bench width of 10 m, which results in an overall slope angle of 44° . The result is steeper than the no-bench scenario, with an overall slope angle of 42° . This geometry produces an estimated overburden volume of 195,123,000 m³, which is smaller than the no-bench scenario of 196,559,500 m³. Therefore, the reduction in stripping volume is 1,436,500 m³ or approximately 0.73%. This study shows that optimizing the bench configuration enables the implementation of steeper overall slope angles while reducing the required stripping volume in open pit mine planning.

Keywords: Slope optimization, slope stability, limit equilibrium method, open pit mining, bench geometry.

1. Introduction

Failure on mining slopes is an event that can cause various losses, both material and non-material (Pasarong, Chaerul and Desi, 2025). For mine workers, slope failure can have a significant impact on their physical, psychological, social, and economic well-being, as well as a decrease in productivity levels (Safitri, Safitri and Alvaro, 2024). In addition, slope failure can also result in financial losses due to the additional costs incurred for handling post-slope failure conditions (Azizi et al., 2019). Then, slope failure in open-pit mines has the potential to eliminate reserves, thereby necessitating the mine's premature closure (Nicholas and Sims, 2000). Losses due to damage to mining equipment can also occur due to slope failure in mines (Kolapo et al., 2022).

Several factors influence slope stability, including groundwater presence, slope geometry design, rock mass condition, geological complexity, and mining operations (Syarbini et al., 2025; Sahya and Misbahuddin, 2026). Mining operations, such as drill and blast operation on rock materials and the use of heavy equipment, also play a role (Hustrulid, McCarter and Van Zyl, 2000). Among these factors, slope geometry design is the most influential on slope stability. This is supported by research that conducted a sensitivity analysis comparing the influence of slope design with other parameters on the slope's factor of safety (Karthik, Manideep and Chavda, 2022).

A gentle slope helps prevent it from failing. (Syafar, 2017; Aisah and Ardiansyah, 2023). This relationship between slope geometry and safety factor has been demonstrated across various geological settings and lithologies, including soil slopes on road embankments (Radityo et al., 2024) and andesite quarry

slopes in volcanic environments (Simatupang, Kausarian and Elizar, 2025). If a slope's height is increased during design, its angle must be reduced to keep it stable (Lee et al., 2009). Reducing the slope angle can linearly increase the stability of the slope, which is represented by the factor of safety value. This had been studied using the finite element method by conducting an analysis process on several slope scenarios where the coefficient value is -0.9761 (Shiferaw, 2021).

Optimal slopes are needed to achieve a compromise between safety and economics. In the mining industry, especially open-pit mining, gentle slopes mean a higher stripping ratio, so more material needs to be stripped to reach reserves (Fleurisson, 2012; Mosquera, 2013; Fleurisson and Cojean, 2014). However, if the decision to increase the slope angle is made without any management related to the potential for slope failure, economic parameters such as Net Present Value (NPV) which should be linear to the increase in slope angle will actually slowly decrease due to the increased risk of slope failure which can have significant economic consequences for the mine (Conteras, 2015).

While the impact of slope geometry on slope stability is well-established (Shiferaw, 2021; Rotaru, Bejan and Almohamad, 2022), research specifically focused on optimizing the vertical placement of benches along the slope height to achieve a defined factor of safety remains scarce. In addition, there are not many studies that treat the position and the width of the bench as interrelated design variables within a mining slope optimization framework (Sobko et al., 2022; Deng et al., 2025). As a result, the quantitative relationship between achieving the factor of safety value by optimizing the slope bench design with the aim of reducing the volume of material removed has not been comprehensively defined. (Bezie et al.,

2024; Deng et al., 2025). Field-based characterization of slope materials and rock mass conditions remains essential for grounding analytical models, as demonstrated by integrated GIS and field validation studies on geologically complex terrains (Hilman, Edo Kharisma Army and Rezki Naufan Hendrawan, 2026). The complexity of this problem is significantly amplified on slopes composed of claystone. This lithology is characterized by its heterogeneous mechanical properties and its inherent sensitivity to changes in slope geometry. Consequently, a robust stability analysis under these challenging conditions demands a method capable of more precisely capturing equilibrium conditions, such as the Morgenstern–Price method (Matius Sesa et al., 2024; Haeriska et al., 2025; Rahmat Rahman, Albertus Juvensius Pontus and Agus Winarno, 2025). This situation indicates the need for an integrated optimization approach to obtain a safe and geometrically efficient bench configuration. This study aims to determine the optimal combination of vertical position and bench width that meets the minimum safety factor criteria while minimizing the volume of material removed on claystone slopes.

The combined optimization of vertical bench location and bench width as interdependent geometric factors inside a claystone slope stability framework utilizing the Morgenstern-Price approach is what makes this study novel. This study quantitatively examines how mixed bench layouts affect both slope safety and excavation efficiency, in contrast to earlier research that primarily assessed slope stability from a single geometric perspective. By striking a balance between waste stripping minimization and geotechnical safety requirements, this method offers a more thorough foundation for open-pit slope geometry design.

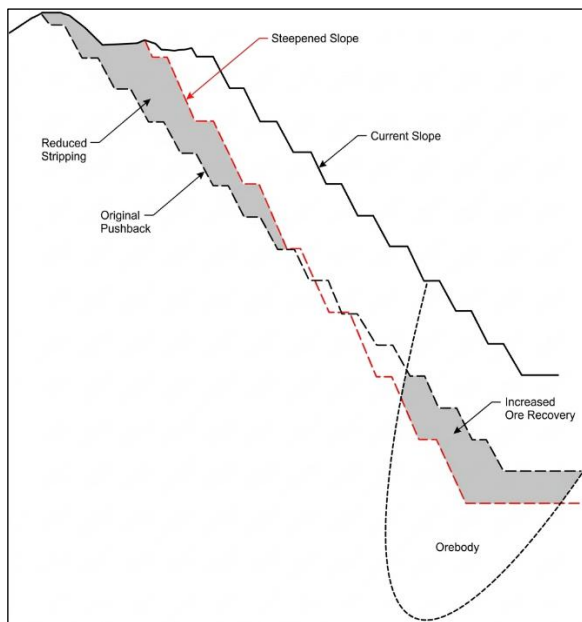


Fig 1. Potential impacts of increasing slope angle (Read and Stacey, 2009).

2. Materials and Methodology

2.1 Slope Geometry Design

Since the failure mechanism was assumed to be a deep-seated slip surface, for which catch benches have minimal impact on the analytical results, the slope geometry design was created using a simplified model that eliminated catch benches from the overall slope geometry. The cross-sections were not derived from actual slope topography and geometry but were based on design parameters determined by the researchers. A

simplified initial slope geometry model was used to isolate and evaluate the influence of vertical bench position and bench width on slope stability. Hence, external factors such as actual topography, geological discontinuity, pore water pressure, and seismic loading were intentionally excluded from the analysis. These parameters included the overall slope height (H), the initial single slope angle (ψ_f), the initial bench width (BW), and the vertical location of the bench along the slope face. The specific values of these parameters determined by the researchers are presented in Table 1.

Table 1. Simple modeling parameters of slope objects

Parameters	Value	Unit
Overall slope height (H)	60	Meters (m)
Initial bench width (BW)	10	Meters (m)
Initial single slope angle (ψ_f)	60	Degrees ($^\circ$)

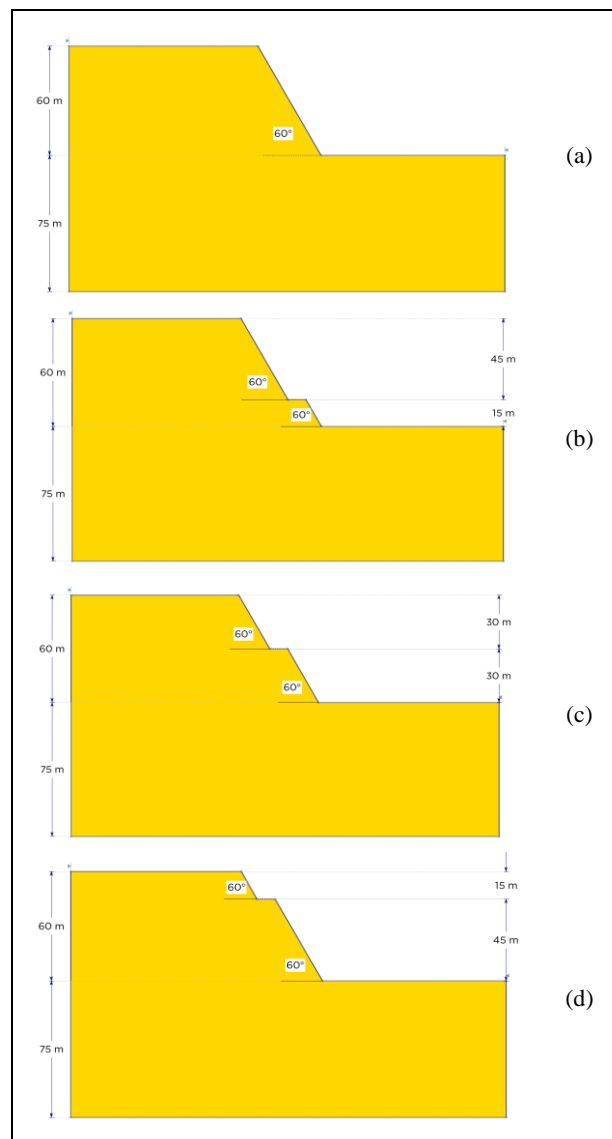


Fig 2. Variations in slope geometry design scenarios with different bench positions and a bench width of 10 meters. (a) slope without bench, (b) slope with a bench position at $\frac{1}{4}$ of the slope height, (c) slope with a bench position at $\frac{1}{2}$ of the slope height, and (d) slope with a bench position at $\frac{3}{4}$ of the slope height.

In this study, four slope geometry design scenarios are used to find the optimal location for positioning bench on the slope. The first scenario involved iterations to determine the safe

overall slope angle and the relative stripping volume compared to a slope geometry design without the addition of a bench. Subsequently, for the second scenario, a similar process was performed on a slope geometry design with a bench added at a height of 15 meters from the slope toe. After that, the third scenario was carried out on a slope geometry design with a bench at a height of 30 meters from the slope toe, and the fourth scenario was carried out on a slope geometry design with a bench at a height of 45 meters from the slope toe. From these four slope geometry design scenarios, researchers will get the influence of the location of the slope bench at heights of $\frac{1}{4}$, $\frac{1}{2}$, and $\frac{3}{4}$ of the total slope height on the overall slope angle and its relative volume. The description of the slope geometry designs can be seen in Figure 2.

Table 2. Common FoS and PoF acceptance criteria values.

Slope scale	Consequences of failure	Acceptance criteria		
		FoS (min) (static)	FoS (min) (dynamic)	PoF (max) P[FoS ≤ 1]
Bench	Low-High*	1.1	NA	25–50%
	Low	1.15–1.2	1.0	25%
Inter-ramp	Moderate	1.2	1.0	20%
	High	1.2–1.3	1.1	10%
Overall	Low	1.2–1.3	1.0	15–20%
	Moderate	1.3	1.05	10%
	High	1.3–1.5	1.1	5%

To determine the optimal bench width, iterations were carried out using several bench width sizes, namely, without a bench (0 m), 5 m, 10 m, 15 m, 20 m, and 25 m. The effect of each change in bench width on the overall slope angle and relative volume was observed at a minimum safety factor threshold of 1.3. The safety factor value of 1.3 is used with the assumption of a static analysis of the overall slope with high consequences (Read and Stacey, 2009). The table of minimum safety factor thresholds can be seen in Table 2 Above.

2.2 Slope Stability Analysis

The analytical method used to assess slope stability is the limit equilibrium method. This limit equilibrium method uses the Morgenstern-Price approach. The Morgenstern-Price limit equilibrium method was chosen because its analysis takes into account all vertical, horizontal, and moment equilibrium states. The Morgenstern-Price method can also be used on all slip surface shapes and has high accuracy in its calculations (Duncan, 1996). The calculations were assisted by a computer program, Slide2 software from Rocscience. The simulations were conducted in static conditions and without groundwater (dry). The slip surface search method used an auto-refine search, assuming the slip surface was circular.

2.3 Material Properties

Table 3. Input parameters of material claystone (Irfan et al., 2023)

Input Parameter	Value	Unit
Natural Density (γ)	17.9523	kN/m ³
Cohesion (c)	20.9	kPa
Internal Friction Angle (ϕ)	40.09	Degrees (°)

The material data utilized in this analysis is secondary data, sourced from research conducted by Irfan et al. (2023). The material employed is claystone, selected for its moderate mechanical properties. This choice allows for the straightforward observation of how geometric factors, such as the overall slope angle, influence the safety factor value. The claystone samples were collected from the Palaubalang Formation, located on Jalan Mugirejo, in the Sungai Pinang District of Samarinda City, East Kalimantan (Irfan et al., 2023).

The input parameters for conducting slope stability analysis use the Mohr-Coulomb failure criterion (Labuz and Zang, 2012). The claystone parameters used can be seen in Table 3.

2.4 Iteration Procedure to Meet Fos Requirement

In the analysis, to obtain a safety factor (SF) of 1.3 for each scenario, an iterative process is carried out on the overall slope angle. First, the model is constructed in accordance with the predetermined initial slope geometry design parameters, after which calculations are performed to obtain the safety factor value. If the resulting safety factor is less than 1, the overall slope angle is reduced in 5-degree increments; if the safety factor approaches or exceeds 1.3, the overall slope angle is adjusted by changing the increment to 0.5 degrees until a value close to, or greater than or equal to, 1.3 is obtained.

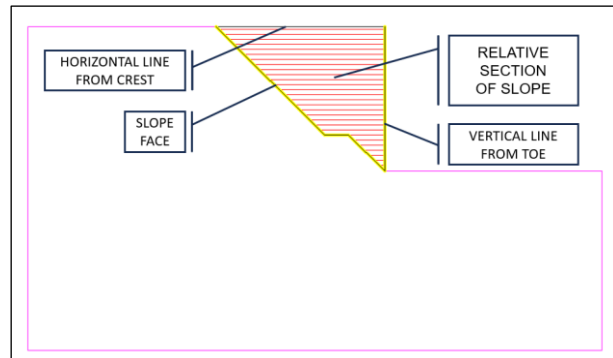


Fig 3. Intended relative cross-section.

2.5 Determining Relative Volume

To determine the relative volume, the relative cross-sectional area of the slope is multiplied by an assumed slope length of 100 m. The relative area is derived from a cross-sectional area defined by the slope face, the vertical line at the slope toe, and the horizontal line at the slope crest. This relative area serves as a metric to compare the size of different cross-sections and the differences arising from various geometric scenarios at FoS values of 1.3. Figure 3 illustrates the intended relative cross-section. ArcGIS software was employed to calculate the cross-sectional area. Specifically, the slope cross-section from the 2D analysis in Slide2 software was exported as a DXF file. This DXF file was then converted into an Esri SHP file. Subsequently, the process was continued within ArcGIS software to obtain the final cross-sectional area.

2.5 Simulation-Based Volume Calculation

After obtaining the relative volume values as outlined in the initial description, a volume simulation will be performed using Geovia Surpac mine planning software. For the simulation, several key parameters are set for several prepared scenarios. A pit 1,000 m wide, 3,000 m long, and 60 m high is simulated. The entire slope edge (toe) is considered the reserve boundary and will not shift. The boundary that will change is the slope crest, which adapts to the slope geometry design. Volume calculations are performed using a block model, which will then be constrained by the pit shell simulation design. Reserves, for example, include coal with a horizontal dip to facilitate analysis of overburden removal volume. In this context, the bottom of the pit shell simulation represents the top of the coal seam.

3. Result and Discussion

3.1 Optimal Bench Position

Scenario 1

In the first scenario, an analysis was carried out on the overall slope without the addition of bench. This scenario

showed that to achieve a stable slope with a minimum safety factor of 1.3, an overall slope angle of 42° is required. With an overall slope angle of 42° and without the addition of bench, the relative cross-sectional area of the slope is $1,973.843 \text{ m}^2$, and assuming the slope length is 100 m, the relative volume is $197,384.3 \text{ m}^3$.

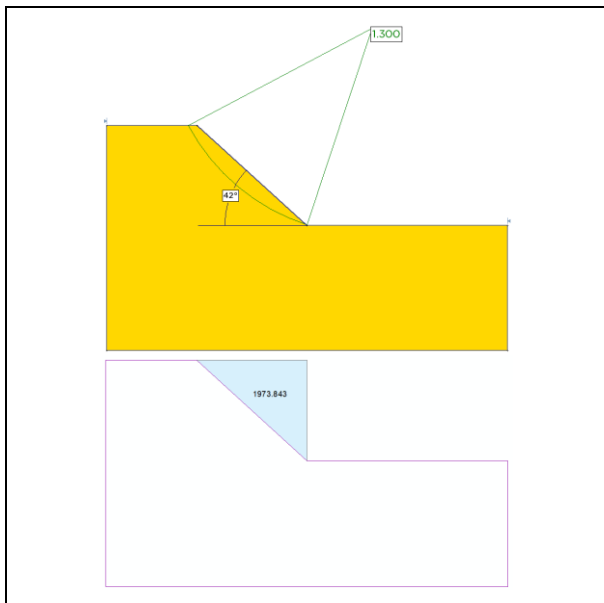


Fig 4. Scenario 1 cross-sectional result

Scenario 2

In the second scenario, a 10 m wide bench was positioned at $\frac{1}{4}$ of the total slope height, i.e. 15 m from the toe elevation of the slope. In order to achieve a safety factor of 1.3, adjustments were made to the overall slope angle. After iterating through several overall slope angle, a stable slope with a safety factor of 1.3 was found at a angle of 40° . The resulting relative cross-sectional area of the slope is $2,268.727 \text{ m}^2$. Assuming a slope length of 100 m, the relative volume is $226,872.7 \text{ m}^3$.

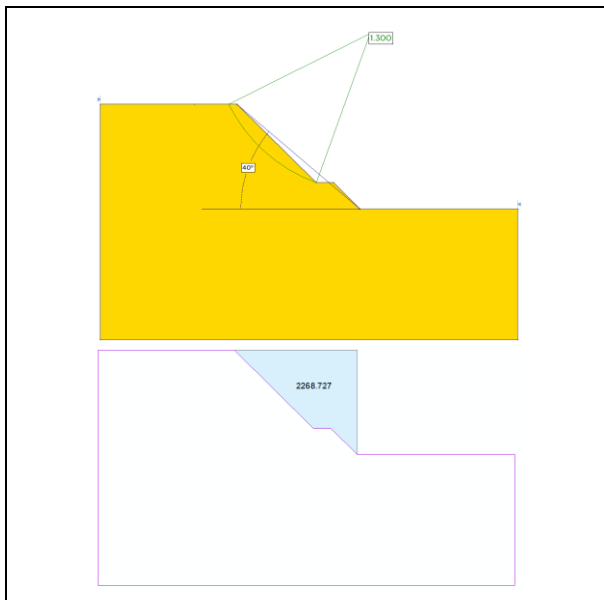


Fig 5. Scenario 2 cross-sectional result

Scenario 3

The third scenario was conducted with a 10 m wide bench positioned at the $\frac{1}{2}$ of the total slope height, i.e. 30 m from the toe of the slope. Iterations were carried out for various overall slope angle, from which the safety factor value closest to and

still greater than 1.3 was obtained. The overall slope angle deemed stable was 44° . With this geometry, the relative cross-sectional area of the slope was found to be $1,873.738 \text{ m}^2$. Assuming the slope length is 100 m, the relative volume is $187,373.8 \text{ m}^3$.

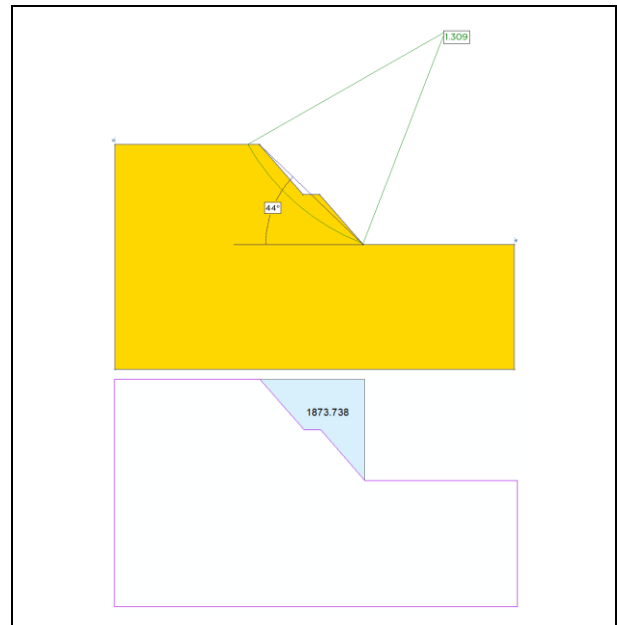


Fig 6. Scenario 3 cross-sectional result

Scenario 4

In the fourth scenario, which was the final scenario to determine the optimal vertical position for the bench, the bench was positioned at the $\frac{3}{4}$ level of the total slope height, i.e. 45 m from the toe of the slope. Iterations were carried out again to achieve a stable slope by testing variations in the overall slope angle. Analysis revealed that to achieve a safety factor value closest to and greater than or equal to 1.3, an overall slope angle of 40° is required. With this overall slope angle, the safety factor value is 1.301. The relative cross-sectional area of the slope obtained is $1,968.727 \text{ m}^2$. Assuming a slope length of 100 m, the relative volume of the slope is $198,872.7 \text{ m}^3$.

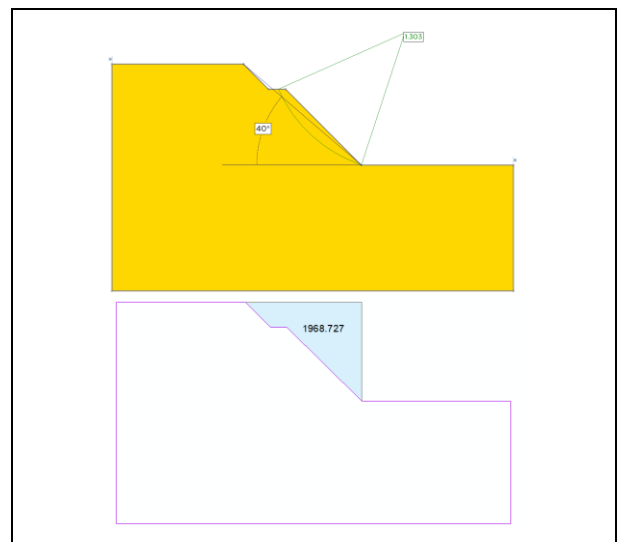


Fig 7. Scenario 2 cross-sectional result.

In summary, the results of the tests to determine the optimal vertical position for the bench on the slope are shown in Table 4 and Figure 5.

Table 4. Relative slope volume and overall slope angle based on the vertical position of the bench on the slope.

Test Scenario	Overall Slope Angle (°)	Volume (m ³)	FoS
1	42	197,384.30	1.300
2	40	226,872.70	1.300
3	44	187,373.80	1.309
4	40	196,872.70	1.303

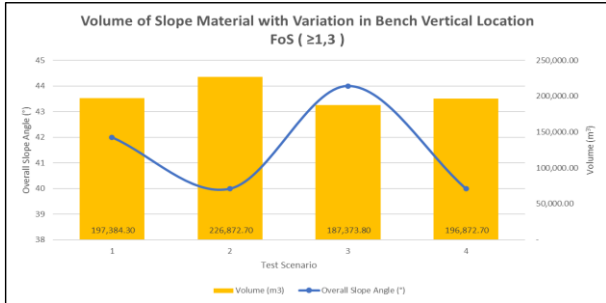


Fig 8. Chart of the slope material volume in the variation of bench vertical position.

Following four tests, which revealed an initial indication of the effect of slope gradient on relative volume, further testing was carried out using a pit shell simulation to determine the excavation volume. The design was carried out in accordance with the procedures outlined in the methodology section. The pit shell design used to calculate the volume of the slope geometry resulting from the tests is shown in the Figure 9.

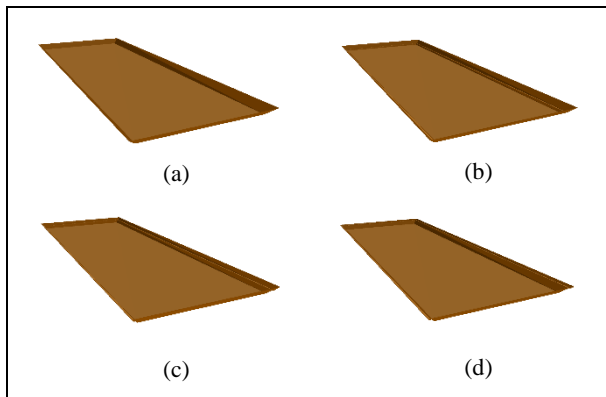


Fig 9. Pit shell of the four bench vertical position scenarios which is (a) without bench, (b) 1/4 of slope height, (c) 1/2 of slope height, and (d), 3/4 of slope height.

The results of the overburden volume estimates from these four pit shell simulations can be seen in the Table 5 and Figure 10.

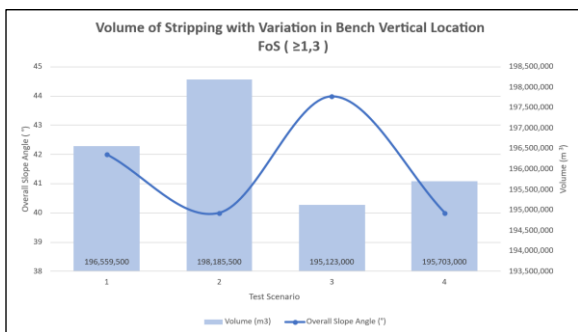


Fig 10. Chart of the simulation-based stripping volume in the variation of bench vertical position.

Table 5. Simulation-based stripping volume and overall slope angle based on the vertical position of the bench on the slope.

Test Scenario	Overall Slope Angle (°)	Volume (m ³)	SF
1	42	196,559,500	1.300
2	40	198,185,500	1.300
3	44	195,123,000	1.309
4	40	195,703,000	1.303

3.2 Optimal Bench Width

Tests to determine the optimal width of the bench were carried out based on the results of the previous test, namely regarding the most optimal vertical position of the bench on the slope. The previous test revealed that the most optimal position for the bench is in the middle of the slope, more precisely at a height of half the total height of the slope. Therefore, tests to determine the optimal width of the bench were carried out on bench positioned in the middle of the slope.

Testing of 0 m Bench Width

For a slope width of 0 m, this can be considered equivalent to the case in scenario 1 of the previous study, i.e. without any bench. From this scenario, the overall slope angle required to achieve a stable safety factor of 1.300 is 42°. The relative cross-sectional area of the slope is 1,973.843 m². Assuming a slope length of 100 m, the relative volume is 197,384.3 m³.

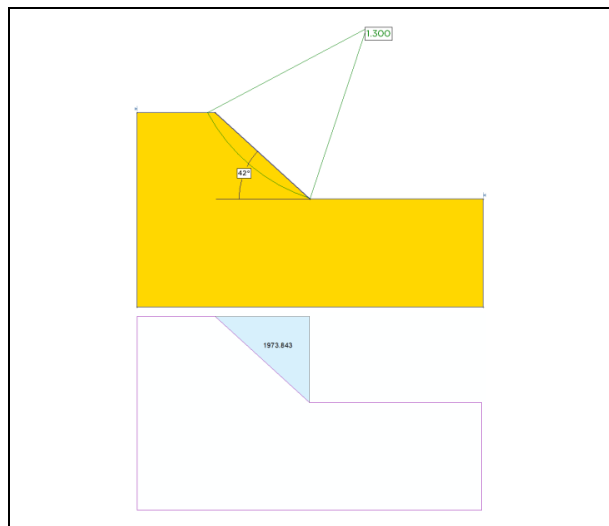


Fig 11. Without bench cross-sectional result.

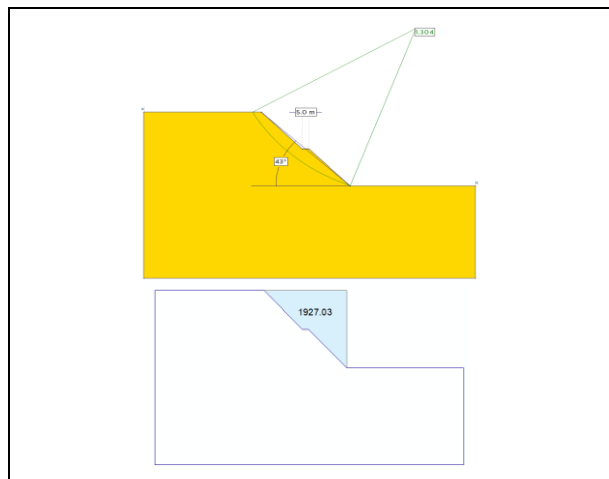


Fig 12. 5 m bench width cross-sectional result.

Testing of 5 m Bench Width

For a slope width of 5 m, the overall slope angle required to achieve a stable safety factor of 1.304 is 43°. The relative cross-sectional area of the slope is 1,927.03 m². Assuming a slope length of 100 m, the relative volume is 192,703 m³ (Fig 12).

Testing of 10 m Bench Width

For a slope width of 10 m, this can be considered equivalent to the case in scenario 3 of the previous test. From this scenario, the overall slope angle required to achieve a stable safety factor of 1.309 is 44°. The relative cross-sectional area of the slope is 1,873.738 m². Assuming a slope length of 100 m, the relative volume is 187,373.8 m³.

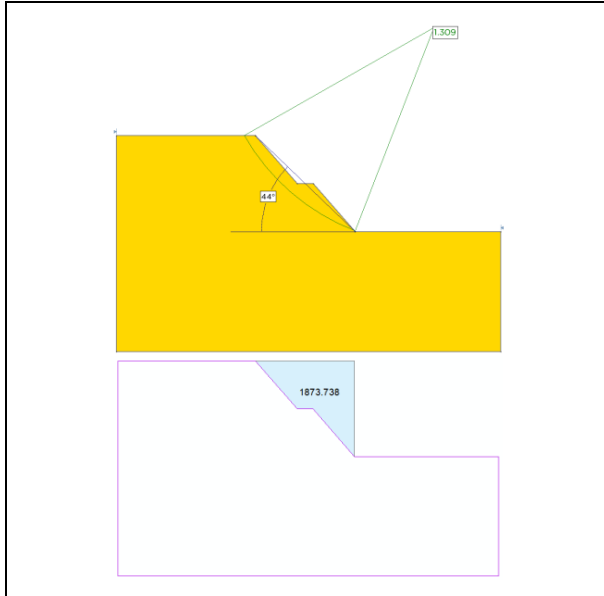


Fig 13. 10 m bench width cross-sectional result.

Testing of 15 m Bench Width

For a slope width of 15 m, the overall slope angle required to achieve a stable safety factor of 1.306 is 42°. The relative cross-sectional area of the slope is 2,006.32 m². Assuming a slope length of 100 m, the relative volume is 200,632 m³.

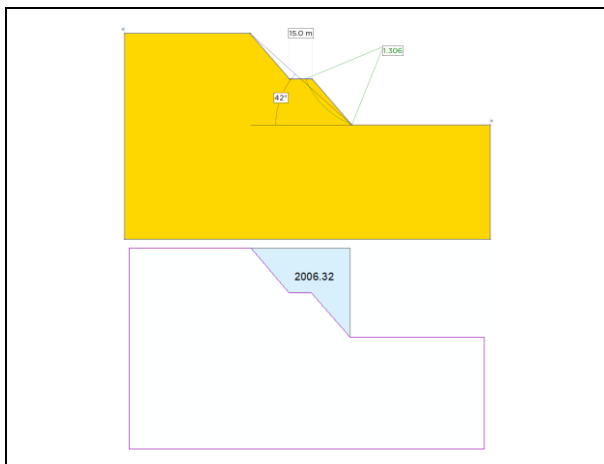


Fig 14. 15 m bench width cross-sectional result.

Testing of 20 m Bench Width

For a slope width of 20 m, the overall slope angle required to achieve a stable safety factor of 1.305 is 40°. The relative cross-sectional area of the slope is 2,154.58 m². Assuming a slope length of 100 m, the relative volume is 215,458 m³.

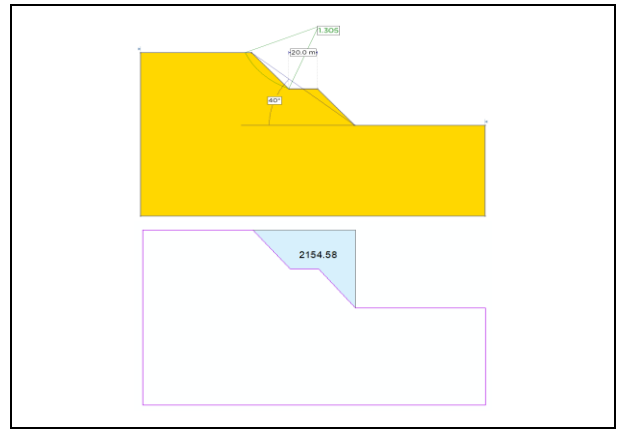


Fig 15. 20 m bench width cross-sectional result.

Testing of 25 m Bench Width

For a slope width of 25 m, the overall slope angle required to achieve a stable safety factor of 1.319 is 38°. The relative cross-sectional area of the slope is 2,331.289 m². Assuming a slope length of 100 m, the relative volume is 233,128.9 m³.

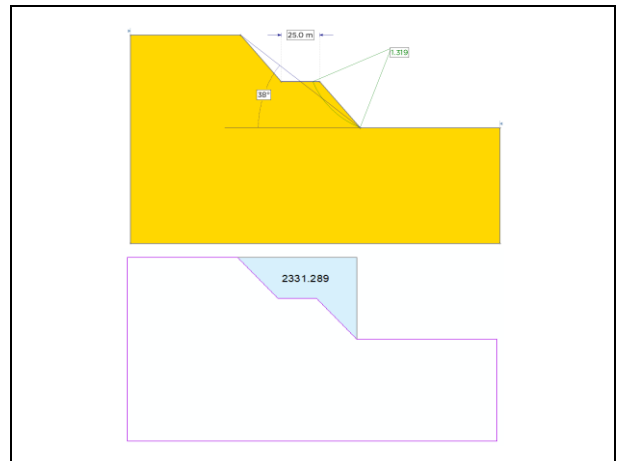


Fig 16. 25 m bench width cross-sectional result.

The results of the tests to determine the optimal bench width are summarized in Table 6 and Figure 17.

Table 6. Relative slope volume and overall slope angle based on the variation of bench width.

Bench Width (m)	Overall Slope Angle (°)	Volume (m ³)	FS
0	42	197,384.30	1.300
5	43	192,703.00	1.304
10	44	187,373.80	1.309
15	42	200,632.00	1.306
20	40	215,458.00	1.305
25	38	233,128.90	1.319

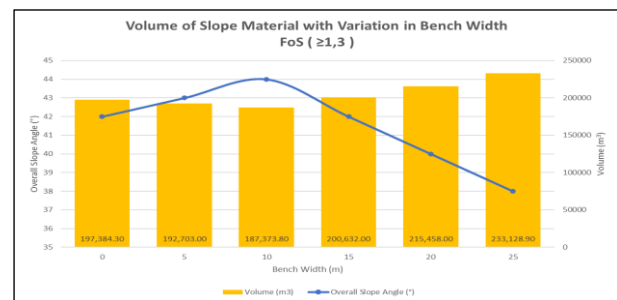


Fig 17. Chart of the slope material volume in the variation of bench width.

Following the completion of six tests, which revealed an initial indication of the effect of bench width on relative volume, further testing was carried out using the same pit shell simulation as in the previous tests to determine the overburden volume. The design was carried out in accordance with the procedures outlined in the methodology section. The pit shell design used to calculate the volume of the slope geometry resulting from the tests is shown in the Figure 18.

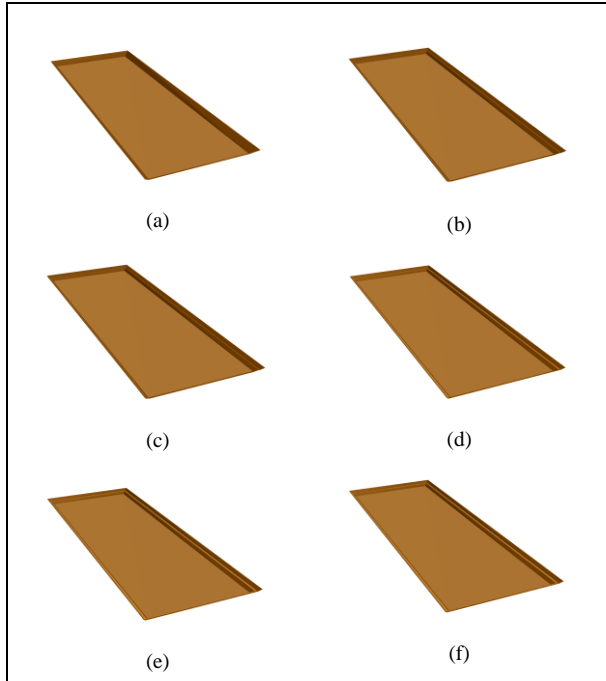


Fig 18. Pit shell of the variation of bench width which is (a) 0 m, (b) 5 m, (c) 10 m, (d) 15 m, (e) 20 m, and (f) 25 m.

The results of the overburden volume estimates from these six pit shell simulations are shown in Table 7 and Figure 19.

Table 7. Simulation-based striping volume and overall slope angle based on the variation of bench width.

Bench Width (m)	Overall Slope Angle (°)	Volume (m ³)	FS
0	42	196,559,500	1.300
5	43	195,691,000	1.304
10	44	195,123,000	1.309
15	42	196,385,000	1.306
20	40	197,653,000	1.305
25	38	198,927,000	1.319

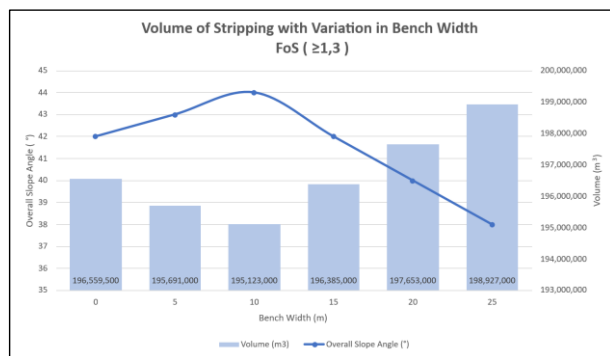


Fig 19. Chart of the simulation-based striping volume in the variation of bench width.

3.3 Discussion

This study conducted tests to determine how bench on a slope can be used to achieve a more optimal slope geometry. Therefore, tests were first carried out to identify the most optimal vertical position for placing bench on the slope. Once this optimal position had been identified, the next step was to determine the width of the bench required to produce the most optimal slope geometry.

The tests carried out revealed several interesting findings. The first concerned the vertical positioning of the bench on the slope. The tests showed that placing the bench in the center of the slope produced the most optimal geometry compared to the other scenarios. Because it effectively interrupted the possible deep-seated failure mass, the bench positioned at $\frac{1}{2}$ of the overall slope height generated the best result. The center part of the slope, where the driving forces and mobilized shear stresses are high, is typically where the critical slip surface passes in deep-seated slope failures. Compared to benches placed close to the toe or crest, placing the bench at the mid-height of the slope minimizes the effective sliding mass and more effectively breaks the continuity of the potential failure surface. This was demonstrated by the fact that the resulting overall slope gradient was the steepest, whilst the volume of material required to form the slope was the smallest. In this study, only a single bench was used. The possibility of testing how the slope responds to variations in the number of benches more than one could be explored in future research.

Based on the results of the pit shell simulation, the scenario without benches yielded an estimated overburden volume of 196,559,500 m³, whilst the configuration with benches placed at half the slope height using 10 m bench width yielded a volume of 195,123,000 m³. Thus, the application of benches at that position results in a reduction in overburden volume of approximately 1,436,500 m³ or around 0.73% compared to the condition without benches. In this study, the pit shell geometry is constrained by the model dimensions of 60 m in height, 3,000 m in length, and 1,000 m in width, so that the pit toe remains constant across all simulation scenarios. Consequently, the volume difference obtained reflects changes in slope geometry efficiency within the same pit geometry boundaries, whilst in pit configurations with different dimensions, the resulting volume difference is likely to vary.

With regard to the optimal bench width, it was found that a bench width of 10 m yielded the most favorable results. The slope's response to an increase in bench width was initially increasingly favorable; this can be seen from the graph, where the volume of material required to form the slope decreased as the bench width increased. However, once the bench width exceeded 10 m, it was found that the overall slope gradient began to level off. This levelling off of the overall slope gradient subsequently resulted in more material needing to be excavated to form the slope. From this, we can see that bench width can influence slope stability and result in a more optimal slope geometry.

It should be emphasized that the 10 m slope width, which was deemed the most optimal in this case, is based on the material properties used. For other material properties, the optimal slope width is not yet known. This could be investigated in future research regarding how slope width affects harder materials such as igneous rock and softer materials such as soil. This would help identify which aspects are most sensitive to the determination of bench width in order to produce a more optimal slope geometry.

Naturally, a simplified slope geometry was used in this test; similar results can be obtained by adding catch benches as well, as shown in Figure 20.

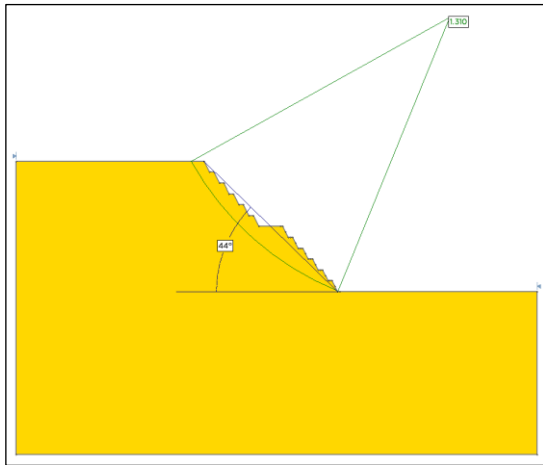


Fig 20. Slope geometry with the addition of a catch bench.

4. Conclusion

This study aims to evaluate the influence of vertical bench position and bench width on slope stability, as well as their implications for the efficiency of excavation volume on slopes composed of claystone. The most optimal position for the bench is at half the total slope height. This configuration results in an overall slope angle of 44° , which is steeper than the 42° angle without bench, whilst still meeting the specified safety factor limits. An analysis of the variation in bench width indicates that a bench width of 10 m is the most optimal configuration for the claystone material conditions in this study. This bench width provides the best balance between slope stability and slope geometry efficiency. The application of the optimal bench configuration resulted in an estimated overburden volume of $195,123,000 \text{ m}^3$, which is lower than the volume of $196,559,500 \text{ m}^3$ in the scenario without benches, leading to a reduction in the simulation-based stripping volume of approximately $1,436,500 \text{ m}^3$, or around 0.73%. The results of this study indicate that optimizing bench configuration—particularly by positioning benches in the middle of the slope with an appropriate width—can improve slope design efficiency by allowing for steeper slope angle whilst reducing the volume of material to be excavated in open-pit mine planning for the same pit geometry.

It is important to take into account the limitations of this study when evaluating the findings. Simplified geometries and homogeneous claystone material properties under dry, static conditions were used to create the slope models. Groundwater pressure, geological discontinuities, material heterogeneity, seismic loading, and actual topographic variations, each one of which could have a substantial impact on slope stability behavior in actual mine were not taken into account in the analyses. Additionally, the slip surface analysis was limited to circular failure mechanisms using the limit equilibrium method. Therefore, the ideal bench configurations found in this work should be understood as preliminary parametric results.

Further research is advised to take into account actual geological and hydrogeological circumstances, such as groundwater pressure, geological discontinuities, heterogeneous material qualities, and seismic loading effects. To increase the usability and dependability of bench optimization techniques in real-world open-pit slope design, more research utilizing probabilistic analysis, three-dimensional slope models, and real mine topography is required.

Acknowledgements

The authors wish to express their sincere gratitude to the Department of Mining Engineering and the Mining Geomechanics Laboratory at Padang State University for the

academic support, facilities and technical assistance provided throughout this research. The authors would also like to thank all those who contributed to the completion of this research through discussions, advice and research support.

References

- Aisah, E. and Ardiansyah, D. (2023) 'Pengaruh Geometri Lereng Terhadap Stabilitas Lereng menggunakan Aplikasi SLOPE/W 2012'. *Jurnal Tekno Global* 12(01), pp. 1–7. Available at: doi:10.36982/jtg.v12i01.3082.
- Azizi, Ahmad, M., Karim, R., Marwanza, I. and Ghifari, M.K. (2019) 'Prediksi Volume Longsoran Tambang Terbuka Nikel Menggunakan Metode Kesetimbangan Batas 3 Dimensi'. *Indonesian Mining Professional Journal* 1(1), pp. 43–48. Available at: https://jurnal.perhapi.or.id/impj.
- Bezie, G., Chala, E.T., Jilo, N.Z., Birhanu, S., Berta, K.K., Assefa, S.M. and Gissila, B. (2024) 'Rock Slope Stability Analysis of a Limestone Quarry in a Case Study of a National Cement Factory in Eastern Ethiopia'. *Scientific Reports* 14(1), p. 18541. Available at: doi:10.1038/s41598-024-69196-8.
- Contreras, L.F. (2015) 'An Economic Risk Evaluation Approach for Pit Slope Optimization'. *Journal of the Southern African Institute of Mining and Metallurgy* 115(7), pp. 607–622. Available at: doi:10.17159/2411-9717/2015/v115n7a7.
- Deng, T., He, J., Sun, J., Peng, S., Pang, X., Chen, T. and Zhang, X. (2025) 'Intelligent Optimization of Slope Step Parameters in Open Pit Mines Containing Weak Interbedded Layers Based on Machine Learning and Multi-Objective Optimization Methods'. *Frontiers in Earth Science* 13, p. 1666375. Available at: doi:10.3389/feart.2025.1666375.
- Duncan, J.M. (1996) 'State of The Art: Limit Equilibrium and Finite-Element Analysis of Slopes'. *Journal of Geotechnical Engineering* 122, pp. 577–596. Available at: doi:10.1061/(ASCE)0733-9410(1996)122:7(577).
- Fleurisson, J.-A. (2012) 'Slope Design and Implementation in Open Pit Mines: Geological and Geomechanical Approach'. *Procedia Engineering* 46, pp. 27–38. Available at: doi:10.1016/j.proeng.2012.09.442.
- Fleurisson, J.-A. and Cojean, R. (2014) 'Error Reduction in Slope Stability Assessment'. *Surface Mining Methods and Technology Systems* 1, pp. 1–41.
- Haeriska, H., Chaerul, M., Desi, N., Harun, A.Muh.Y., Erniati, E. and Marzuki, I. (2025) 'Evaluation of Slope Stability in Mining Areas Using the Morgenstern Price Method'. *Journal La Multiapp* 6(6), pp. 1347–1364. Available at: doi:10.37899/journallamultiapp.v6i6.254.
- Hilman, Z., Edo Kharisma Army and Rezki Naufan Hendrawan (2026) 'Slope Stability Analysis Through the Application of Digital Imagery and Field Validation Using SMR and Q-Slope Methods: A Case Study of Bandar Lampung City, Indonesia'. *Journal of Geoscience, Engineering, Environment, and Technology* 11(1), pp. 1–8. Available at: doi:10.25299/jgeet.2026.11.1.20520.
- Hustrulid, W.A., McCarter, M.K. and Van Zyl, D.J.A. (2000) *Slope Stability in Surface Mining*. Littleton, CO, USA: Society for Mining, Metallurgy, and Exploration.
- Irfan, Trides, T., Winarno, A., Litha Respati, L. and Dina Devy, S. (2023) 'Studi Perbandingan Nilai Kuat Geser Batu Lempung Berdasarkan Kondisi Jenuh, Kondisi

- Natural, Dan Kondisi Kering Formasi Palau Balang Menggunakan Metode Direc Shear Di Kalimantan Timur (Comparative Study Of Clastone Shear Strength Value Based On Saturated Conditions, Natural Conditions, And Dry Conditions Of The Palau Balang Formation Using The Using The Direct Shear Method In East Kalimantan)'. *Journal Scientific of Mandalika (JSM)* 4(5). Available at: <http://ojs.cahayamandalika.com/index.php/jomla/issue/archive>.
- Karthik, A.V.R., Manideep, R. and Chavda, J.T. (2022) 'Sensitivity Analysis of Slope Stability Using Finite Element Method'. *Innovative Infrastructure Solutions* 7(2), p. 184. Available at: doi:10.1007/s41062-022-00782-3.
- Kolapo, P., Oniyide, G.O., Said, K.O., Lawal, A.I., Onifade, M. and Munemo, P. (2022) 'An Overview of Slope Failure in Mining Operations'. *Mining* 2(2), pp. 350–384. Available at: doi:10.3390/mining2020019.
- Labuz, J.F. and Zang, A. (2012) 'Mohr–Coulomb Failure Criterion'. *Rock Mechanics and Rock Engineering* 45(6), pp. 975–979. Available at: doi:10.1007/s00603-012-0281-7.
- Matius Sesa, H., Najib, N., Luthfi Dalimunthe, H. and Handietri, Z. (2024) 'Slope Stability Evaluation and Geometrical Recommendation Using The Morgenstern Price Method'. *Jurnal Teknologi* 16(1), p. 53. Available at: doi:10.24853/jurtek.16.1.53-64.
- Mosquera, J. (2013) *Static and Pseudo-Static Stability Analysis of Tailings Storage Facilities Using Deterministic and Probabilistic Methods*. Montréal, QC, Canada: McGill University.
- Nicholas, D.E. and Sims, D.B. (2000) 'Collecting and Using Geological Structure Data for Slope Design'. in Hustrulid, W. A., McCarter, M. K., and Van Zyl, D. J. A. (eds.) *Slope Stability in Surface Mining*. Golden, CO, USA: Society for Mining, Metallurgy, and Exploration
- Pasorong, E.P., Chaerul, M. and Desi, N. (2025) 'Pemetaan Resiko Bencana Longsor Menggunakan Sistem Informasi Geografis (SIG) pada Jalan Tambang PT. Ifishdeco, Tbk'. *Jurnal Teknik* 5(1)
- Radityo, D., Bilal Al Farishi, Rezky Naufan Hendrawan, Alviyanda and Imam Ahmad Sadisun (2024) 'Slope Stability Analysis Throughout Road Around Bukit Barisan Selatan National Park (BBSNP) using Fellenius Method'. *Journal of Geoscience, Engineering, Environment, and Technology* 9(3), pp. 279–286. Available at: doi:10.25299/jgeet.2024.9.3.14902.
- Rahmat Rahman, Albertus Juvensius Pontus and Agus Winarno (2025) 'Pengaruh Parameter Geoteknik Hasil Pengeboran terhadap Desain Tambang di PT. Insani Baraperkasa, Kutai Kartanegara'. *Globe: Publikasi Ilmu Teknik, Teknologi Kebumihan, Ilmu Perkapalan* 3(2), pp. 17–31. Available at: doi:10.61132/globe.v3i2.788.
- Read, J. and Stacey, P. (2009) *Guidelines for Open Pit Slope Design*. 1st edn. Canberra, Australia: CSIRO Publishing.
- Rotaru, A., Bejan, F. and Almohamad, D. (2022) 'Sustainable Slope Stability Analysis: A Critical Study on Methods'. *Sustainability* 14(14), p. 8847. Available at: doi:10.3390/su14148847.
- Safitri, O., Safitri, M. and Alvaro, R.R. (2024) 'Manajemen Risiko pada Sektor Pertambangan Informal: Analisis Longsor Tambang Emas Ilegal di Nagari Sungai Abu, Hiliran Gumanti, Solok pada Tahun 2024'.
- Sahya, M.M.Z. and Misbahuddin (2026) 'Analysis of the Factor of Safety (FS) in Slope Stability Against Blasting Activities at Pit X, South Kalimantan'. *Journal of Geoscience, Engineering, Environment, and Technology* 10(4), pp. 1–11. Available at: doi:10.25299/jgeet.2025.10.1.1.24084.
- Shiferaw, H.M. (2021) 'Study on the Influence of Slope Height and Angle on the Factor of Safety and Shape of Failure of Slopes Based on Strength Reduction Method of Analysis'. *Beni-Suef University Journal of Basic and Applied Sciences* 10(1), p. 31. Available at: doi:10.1186/s43088-021-00115-w.
- Simatupang, I.D., Kausarian, H. and Elizar (2025) 'Geotechnical Insights into Andesite Quarry Slope Stability: A Case Study from Desa Usul, Indragiri Hulu, Riau, Indonesia'. *Journal of Geoscience, Engineering, Environment, and Technology* 9(04), pp. 591–599. Available at: doi:10.25299/jgeet.2024.9.04.20074.
- Sobko, B.Y., Lozhnikov, O. V, Chebanov, M.O. and Vinivitin, D. V (2022) 'Substantiation of the Optimal Parameters of the Bench Elements and Slopes of Iron Ore Pits'. *Naukovyi Visnyk Natsionalnoho Hirnychoho Universytetu* (5), pp. 26–32. Available at: doi:10.33271/nvngu/2022-5/026.
- Syafar, Z. (2017) 'Analisis Kestabilan Lereng Dengan Metode Bishop Pada Penambangan Nikel'. *Jurnal Geomine* 4(3), pp. 90–93. Available at: doi:10.33536/jg.v4i3.70.
- Syarbini, K. et al. (2025) 'Sensitivity Analysis of Phase 5 Batu Hijau Pit Walls'. *Journal of Geoscience, Engineering, Environment, and Technology* 10(2)



© 2026 Journal of Geoscience, Engineering, Environment and Technology. All rights reserved. This is an open access article distributed under the terms of the CC BY-SA License (<http://creativecommons.org/licenses/by-sa/4.0/>).